Unlocking the Potential of *Phaseolus Vulgaris* Particulates on AA6063 Alloy for Enhanced Mechanical, Corrosion and Opto-electrical Performance

A. D. Adeleye[1], O. S. I. Fayomi[1, 2] and J. O. Atiba[1*]

[1]Department of Mechanical Engineering, Bells University of Technology, Ota, Ogun State, Nigeria
[2]Department of Mechanical Engineering Science, University of Johannesburg, Johannesburg, South Africa
Corresponding authors: atibajoshua7@gmail.com

Abstract

AMMC are notable for their extensive research and unique property profiles, surpassing those of traditional solid metals. Their remarkable strength sets them apart, making them highly sought-after and versatile across diverse industries. The integration of reinforcements into AMMC boosts their properties, including increased tensile and compressive strength, improved wear resistance, reduced thermal expansion and enhanced hardness, characteristics unattainable with conventional materials. However, the use of CMC, such as SiC and Al_2O_3, escalates the production cost of AMMC, thereby limiting their application in various industries. In recent times, researchers have increasingly turned to natural reinforcements derived from waste sources, such as bamboo leaves, rice and palm kernel shells. However, investigations into PV potential as reinforcements for AMMC have been limited, prompting the initiation of this study. This research aimed to examine mechanical, microstructural, electrochemical and optoelectronic properties of AMMC reinforced with PVP. The study demonstrated an increase in hardness values, from 28.1 to 38.5 HRB, with 25% PVP reinforcement, and a significant reduction in CR, from 12.06 to 6.13 mm/yr. Electrical resistivity and conductivity measurements showed variations across composite samples, while microstructural analysis confirmed uniform PVP dispersion and integration within the metal matrix, alongside additional crystalline formations.

Keywords: Al; corrosion; HRB; optoelectrical; PV; PVP; reinforcement.

Introduction•

Many engineering materials in today's world require properties such as increased strength, weight reduction and cost-effectiveness, particularly in terms of energy usage. The search for such materials arises from the aim to produce lightweight structural elements and engine parts with high strength-to-weight ratios, hence reducing excessive fuel consumption and CO_2 emissions [1-4]. Due to rigorous demands of engineering applications, materials must exhibit a range of complex

---

•The abbreviations list is in page 361.

properties, including high strength, exceptional wear resistance, improved corrosion resistance and other desirable mechanical, electrical and chemical characteristics. However, it is rare to find all these properties in a single metallic material. Researchers have found that achieving such desirable features is only possible through merging different materials, to create a combination with enhanced properties [5-7].

The combined materials are commonly known as composites, which have the unique potential to improve selected characteristics of monolithic materials, while remaining superior to their counterparts. They are generally classified according to the composition of their base matrix phase: CMC, MMC and PMC [8-12]. MMC are highly engineered materials renowned for their ability to blend diverse properties by combining matrices with hard particulate reinforcements, thereby attaining substantial engineering and industrial importance compared to traditional metallic alloys. Within the spectrum of MMC, AMMC are notable for their extensive unique property profiles, surpassing those of traditional solid metals. Their remarkable strength sets them apart, making AMMC highly sought-after and versatile across diverse industries [13-15].

AMMC efficiency relies on various factors impacting their properties, such as type, volume and weight fraction, as well as particle size, distribution and shape of reinforcements. Additionally, production method employed also significantly influences overall effectiveness of composites [16-19]. Research of those factors reveals that reinforcements play a key role in sustainable AMMC. In manufacturing, AMMC, such as Al-Si, Al-Cu and Al-Si-Mg, serve as MMC, while reinforcements like SiC, Al_2O_3, C, B, B_4C, AlN, SiO_2 and BN are incorporated into them. Specifically, the integration of reinforcements into Al matrixes enhances their properties, including increased tensile and compressive strength, improved wear resistance, reduced thermal expansion and greater hardness, characteristics unattainable with conventional materials [20-22]. However, the use of CMC such as SiC and Al_2O_3 escalates the production cost of AMMC, thereby limiting their application in various industries [23].

Thus, researchers have been investigating alternate reinforcement materials with the aim of cutting AMMC production costs. These studies have revealed an array of naturally occurring particles, including agro-waste and industrial by-products, showing promise as feasible alternatives to typical reinforcements in AMMC. Given its abundance and economic viability, agrowaste has emerged as an especially favourable reinforcement material. Extensive research efforts on diverse agricultural by-products have revealed their intrinsic richness in Si and Mg, making them potential reinforcing possibilities [24]. The realm of agrowaste presents a promising avenue for exploring particulate reinforcements. It offers a dual benefit of addressing pollution challenges and enhancing the strength of metal matrices. In recent times, researchers have increasingly turned to natural reinforcements derived from waste sources such as bamboo leaves [25-28], rice husk [29-31] and palm kernel shells [32-36]. However, investigations into the potential of PV shells as reinforcements for AMMC have been limited, prompting the initiation of this study.

Thus, the primary objective of this research was to examine mechanical, microstructural, electrochemical and optoelectronic properties of AMMC reinforced with PVP.

Research methodology

Al alloy (AA6063), which was sourced locally from the metal market, served as base material. PVP were prepared by cleansing them with acetone and warm water, air-drying for 48 h, crushing, milling and sieving, to achieve the desired particle size of 45 µm. Final particulate size can be observed in Fig. 1.

Figure 1: Photo of PVP sample.

Chemical compositions of AA6063 and PVP, after characterization, are detailed in Tables 1 and 2, respectively.

Table 1: Chemical composition of AA6063.

Elements	Fe	Cu	Mg	Mn	Si	Ti	Zn	Cr	Al
%Wt.	0.11	0.01	0.79	0.02	0.88	0.008	<0.01	<0.01	Bal.

Table 2: Chemical composition of PVP.

Compound Ct	CaO	Al_2O_3	K_2O	P_2O5	$SiO2$	MgO	Fe_2O_3	MnO	Na_2O
(wt%)	41.21	15.43	7.32	2.39	15.69	4.85	9.71	0.72	1.76

Stir casting technique was employed to fabricate Al metal matrix composite. This method involved uniformly mixing the reinforcement into the matrix material, using a mechanical stirrer and pouring the composite mix into the desired mould geometry. Five samples were prepared with varying wt.% of PVP (0, 10, 15, 20 and 25%), following ASTM B179 standard specifications. For mechanical assessment, HRB was measured employing an HR-150A HRB testing machine (ASTM E18-22). Samples were indented for 10 secs, at a force of 5 kg, with multiple measurements taken to ensure accuracy. Corrosion testing utilized an AUTO LAB potentiostat galvanostat (PGSTAT 101), in a 1 M HCl environment with a three-electrode polarization setup employing Ag/AgCl and graphite electrodes. Microstructural analysis was conducted using a JOEL JSM-7600F machine for SEM/EDXS, and Rigaku D/Max-llC X-ray diffractometer for XRD experiments. Electrical conductivity and resistivity were assessed using a custom electrical setup (Fig. 2)

[37]. Fig. 3 shows the empirical electrical setup used to investigate magnetic permeability of the composite, in response to inductive change.
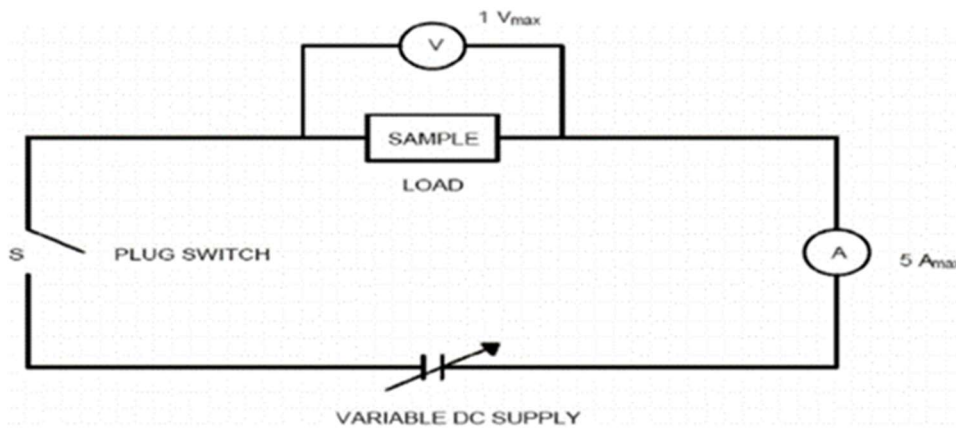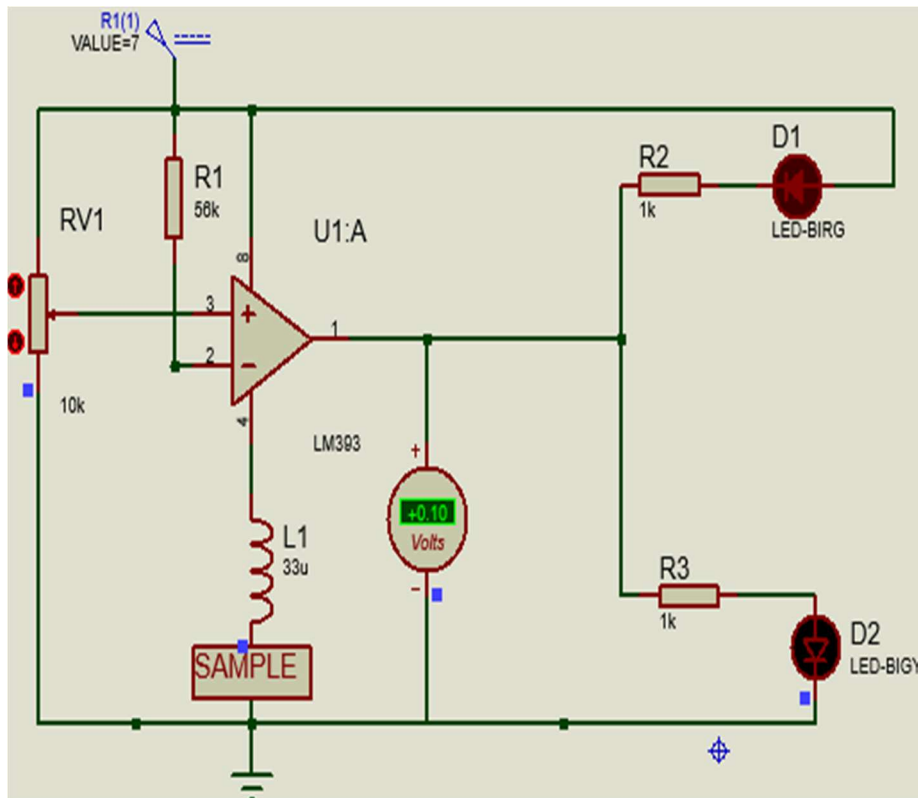

Figure 2: Experimental electrical setup [37].

Figure 3: Magnetic saturation test circuit.

Results and discussion
Hardness values of samples
HRB value of the developed composites is shown in Fig. 4. According to HRB readings, the samples with highest Ct of PVP showed the greatest reading and helped raise the substrate material's hardness from 28.1 to a final composite deposition of 38.5 HRB. Overall, there was an increase in hardness values for samples containing different PVP sizes, from 5.33 to 37.01%. The enhanced

strength observed in the fabricated composites can be largely attributed to robust interfacial bonding and adhesion between soft and ductile AA6063 matrix and PVP reinforcement. This bonding significantly augmented load-bearing capacity of the composite, thus minimizing matrix deformation. Additionally, uniform dispersion of reinforcements within matrix phase contributed to observed results [23, 38, 39]. However, it should not be assumed that increasing the Ct of particulate reinforcements will consistently lead to more hardness, as this is limited by the availability of intermetallic ions required for bonding with the lattice [31].
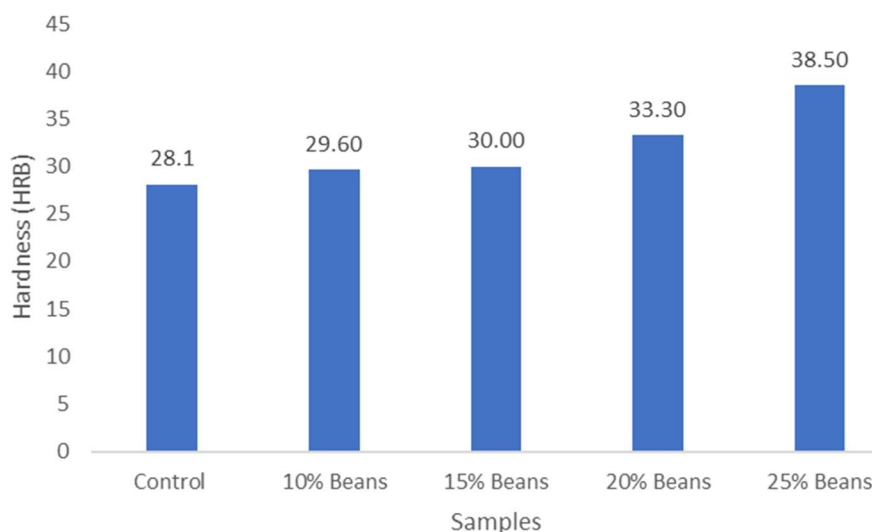

Figure 4: Hardness values of samples.

Corrosion evaluation of samples

Table 3 indicates results of polarization test and Tafel plot in terms of CR, J_{corr}, E_{corr} and R_p.

Table 3: Tafel plots of samples.

Samples	E_{corr} (V)	J_{corr} (A/cm²)	CR (mm/yr)	Rp (Ω)
Control	-0.383	2.01E-02	12.06	3.58E+01
10% PVP	-0.381	1.77E-02	10.34	4.02E+01
15% PVP	-0.394	1.57E-02	9.31	3.88E+01
20% PVP	-0.416	1.69E-02	8.63	3.44E+01
25% PVP	-0.442	1.75E-02	6.13	5.42E+01

In the presence of Cl⁻ ions, the control sample corroded rapidly, with a CR of 12.06 mm/yr compared to Al with 25% PVP sample, which had the lowest CR of 6.13 mm/yr. Similar reduction trend in CR values from reinforced samples was observed as the Ct of PVP increased from 10 to 25%, gaining a 41% decrease in CR. This confirms the inherent inhibitive nature of PVP. Fig. 5 shows corrosion response stability throughout each composite sample during a 120 secs.

timeframe. The plot shows that the sample without PVP reinforcement consistently had the highest potential across the 120 secs. period. This specimen had the most noticeable shift towards the positive region, indicating a higher potential. In contrast, samples with different Ct of PVP showed lower values, shifting towards negative potential range. Notably, the specimen with 20% PVP reinforcement had the lowest potential, lower than -0.5 V. The curve's flow towards the negative region indicates that PVP had more impact on the cathodic than on the anodic reaction, implying that it was cathodic inhibitory [40-42].
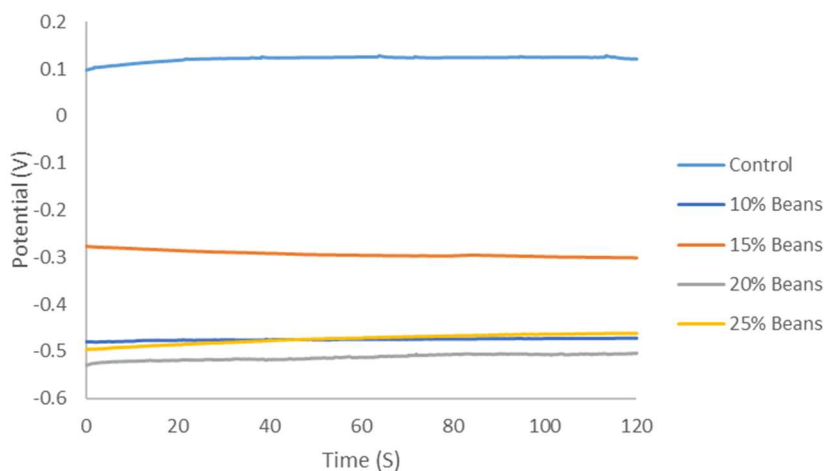
Figure 5: OCP plots of PVP samples.

The influence of corrosion polarization's cathodic effect is further elucidated in Fig. 6, which showcases a decrease in both cathodic reactions of sample corrosion, as the reinforcement Ct increased from 10 to 25 wt.%.
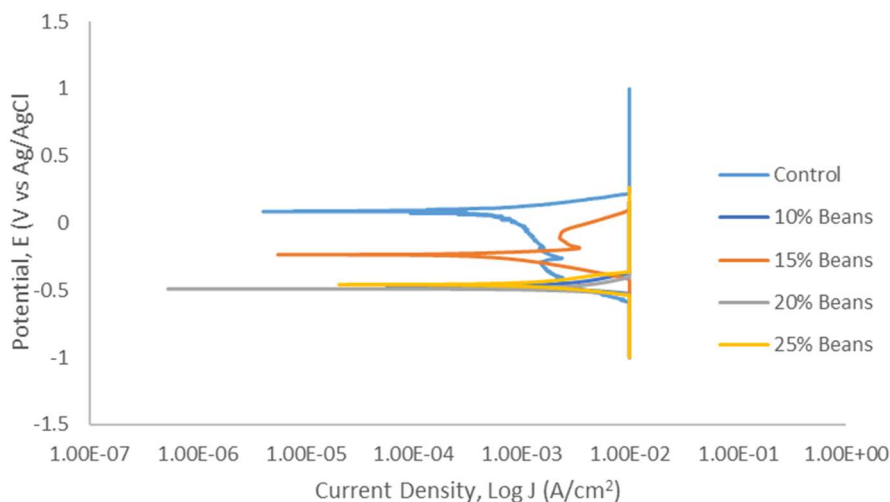
Figure 6: PVP samples plots.

Opto-electrical response of the samples

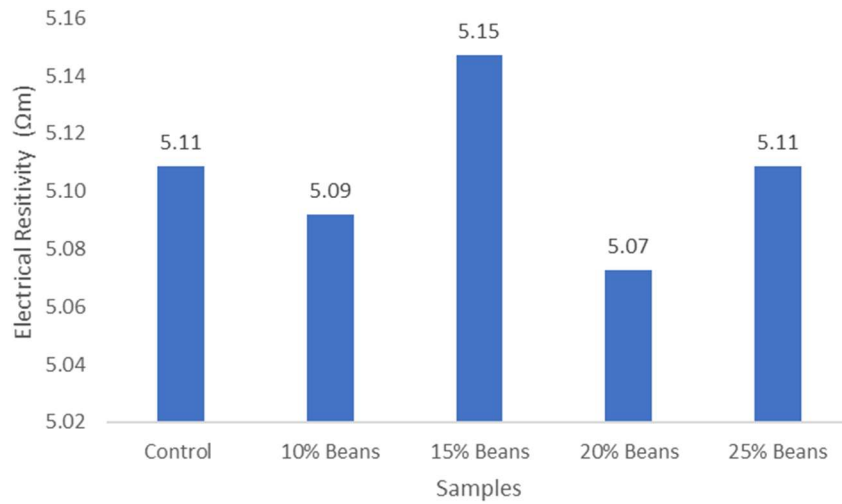Figs. 7 and 8 depict the results of electrical resistivity and conductivity for the produced coating samples.

Figure 7: Electrical resistivity of composite samples.

Interestingly, the trend in electrical resistivity did not follow a uniform pattern, as the results show a paired array, with the control and the most reinforced sample exhibiting the same resistivity value of 5.11 Ωm, while 10 and 20% reinforced samples had similar values of 5.09 and 5.07 Ωm, respectively (Fig. 8).
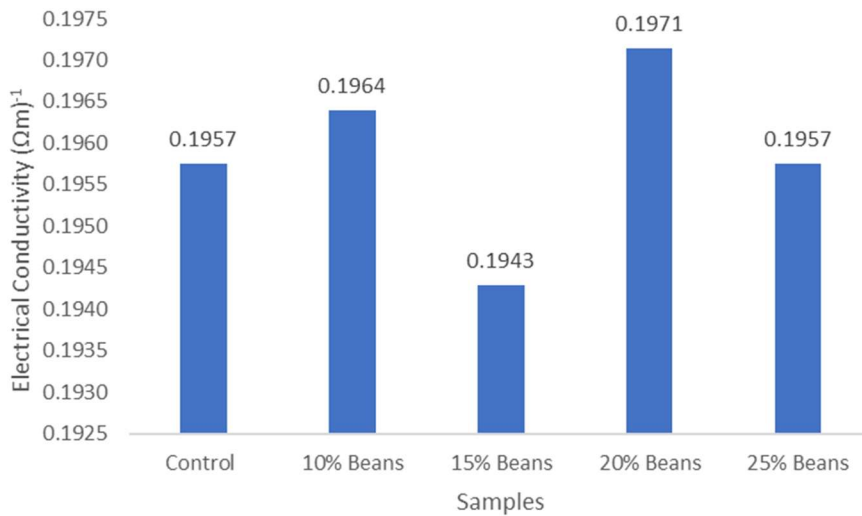

Figure 8: Electrical conductivity of composite samples.

Conversely, a reverse pattern was observed for conductivity plots, with the control and the most reinforced sample having the same conductivity value of 0.1957 Ωm^{-1}, while 10 and 20% reinforced samples had similar values of 0.1964 and 0.1971 Ωm^{-1}, respectively. However, 15% PVP sample exhibited highest conductivity of 0.1943 Ωm^{-1}. Contrary to expectations based on prior research studies, this study revealed a deviation attributed to non-uniform distribution of PVP across Al matrix [37, 43, 44]. Magnetic permeability response of the samples is shown in Fig. 9. Al, unlike Fe, is not ferromagnetic, which corresponds to its low magnetic permeability. Experimental investigation aimed at assessing the influence of PVP on specimens' enhancement revealed a

negligible alteration in metal ferromagnetism, evidenced by voltage variation across diverse samples with increasing inductance, which amounted to a total voltage change of merely 0.17 V in the most reinforced sample.
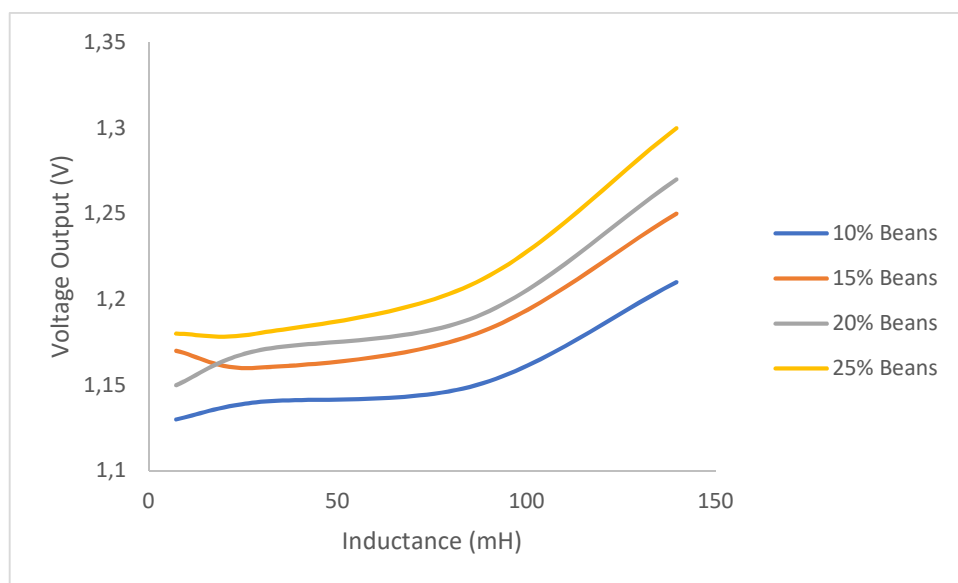

Figure 9: Magnetic permeability response of the samples.

Microstructural analysis of samples

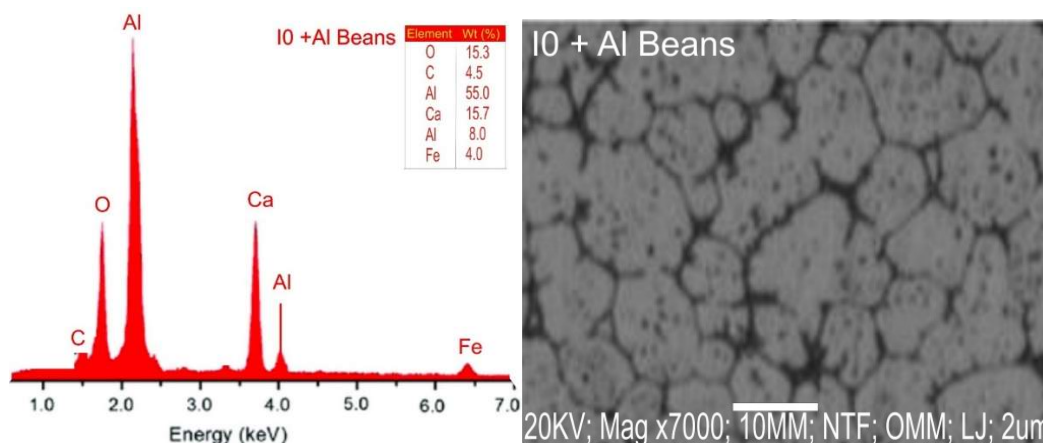SEM micrographs and EDXS analysis of composites with lowest reinforcement Ct (10% PVP) are depicted in Fig. 10.

Figure 10: SEM/EDXS of 10% PVP samples.

From SEM images, it is evident that PVP adequately dispersed within the matrix, allowing for visualization of grain boundaries and pores throughout Al matrix. EDXS spectra indicate peaks corresponding to Al, Ca, Si, Mg, C and O, which confirmed that CaO, SiO_2 and Al_2O_3 were major constituents of the reinforcements, as confirmed by PVP characterization. Additionally, oxygen

presence suggests its contribution for silica phase of PV. Similar observations have been reported by previous studies [29, 45].

Fig. 11 presents SEM/EDXS morphology of 25% PVP sample. Analysis of SEM images indicate PVP agglomeration in certain regions of the base matrix, resulting in a reduction in distinct grain boundaries and an increase in porous areas across the matrix.
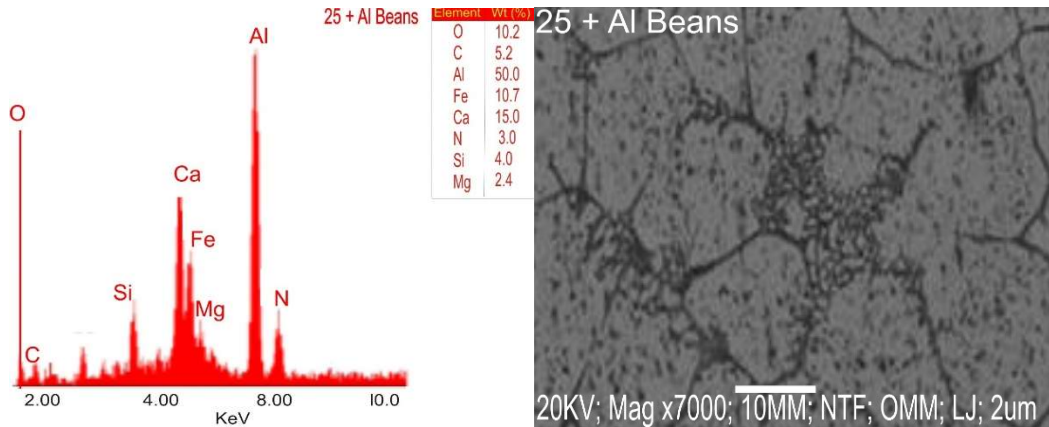

Figure 11: SEM/EDXS of 25% PVP samples.

Figs. 12 and 13 show XRD profiles of 10 and 25% PVP samples, respectively. The plots analysis reveals the highest characteristic diffraction peaks for Al-Si based compound (AlZnS$_2$), in both PVP samples, at $2\theta = 39°$ and $2\theta = 108°$. These peaks correspond to the substantial integration of PVP within the MMC. Furthermore, a range of additional crystalline formations was observed across diverse phases, including Al(Mn), Ca(Zn), Mg(Si) and Mg(Zn), which provides evidence supporting the enhancement of corrosion resistance, strengthened adhesion and refined surface conditioning.

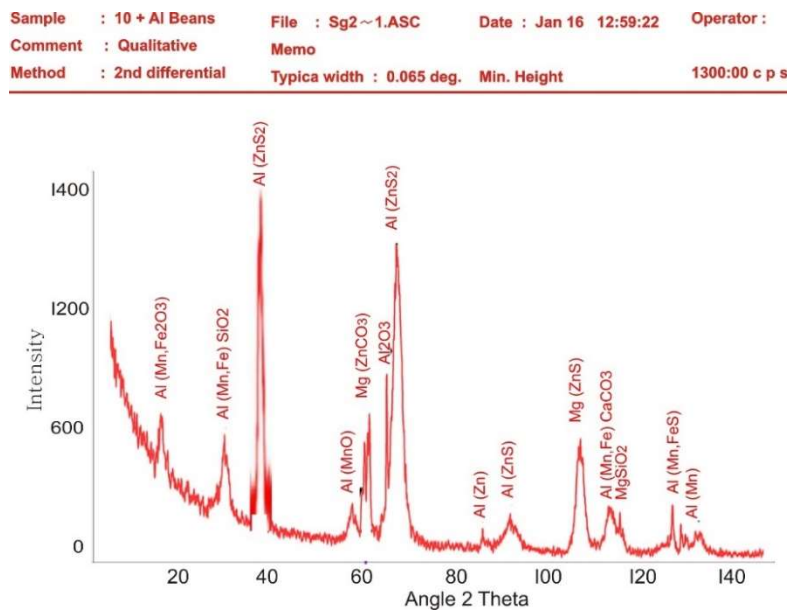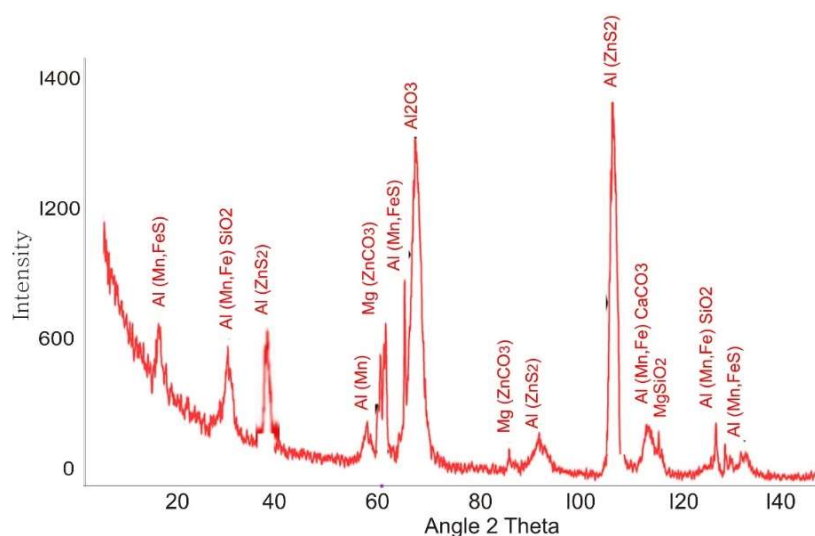**Figure 12**: XRD of coated samples (10% PVP).

Figure 13: XRD of developed sample (25% PVP).

Conclusion

In conclusion, the study revealed notable findings across various experiments. HRB test demonstrated an average increase in hardness values from 28.1 HRB, for the control sample, to 38.5 HRB for the composite containing 25% PVP. CR values from for control and composite samples with 25% PVP were 12.06 and 6.13 mm/yr, respectively, which is a substantial decrease. Electrical resistivity and conductivity measurements showed intriguing deviations from expected trends: resistivity values shifted from 5.07 to 5.11 Ωm; and conductivity values changed from 0.1943 to 0.1971 Ωm^{-1}, across different composite samples. Microstructural analysis confirmed uniform dispersion of PVP within the matrix, with SEM/EDXS and XRD analyses highlighting its integration within the MMC, and the presence of additional crystalline formations. Overall, these results underline PVP potential as an effective AMMC reinforcement, offering promising prospects for the development of lightweight and high-strength materials with reduced environmental impact and production costs.

Acknowledgments

Competing interests

The authors declare no competing interests.

Authors' contributions

A. D. Adeleye: writing of manuscript and figures. **O. S. I. Fayomi**: research supervision. **J. O. Atiba**: writing of manuscript and tables.

Abbreviations
Al_2O_3: aluminum oxide
AMMC: aluminum metal matrix composites
ASTM: American Society for Testing and Materials
CMC: ceramic matrix composites
CR: corrosion rate
Ct: concentration
E_{corr}: corrosion potential
EDXS: energy dispersive X-ray spectroscopy
HCl: hydrogen chloride
HRB: hardness Rockwell B
J_{corr}: corrosion current
MMC: metal matrix composites
PMC: polymer matrix composites
PV: *Phaseolus vulgaris* (bean shell)
PVP: *Phaseolus vulgaris* particulates
R_p: polarization resistance
SEM: scanning electron microscopy
SiC: silicon carbide

References

1. Shen J, Yin W, Wei Q et al. Effect of ceramic nanoparticle reinforcements on the quasistatic and dynamic mechanical properties of magnesium-based metal matrix composites. J Mater Res. 2013;28(13):1835-52. https://doi.org/10.1557/jmr.2013.16

2. Pramanik A, Littlefair G. Fabrication of nano-particle reinforced metal matrix composites. Adv Mater Res. 2013;651:289-94. https://doi.org/10.4028/www.scientific.net/AMR.651.289

3. Tjong SC. Processing and deformation characteristics of metals reinforced with ceramic nanoparticles. In: Nanocrystalline materials. Elsevier. 2014:269-304. https://doi.org/10.1016/B978-0-12-407796-6.00008-7

4. Olufunmilayo JO, Babaremu KO. Agricultural waste as a reinforcement particulate for aluminum metal matrix composite (AMMCs): A review. Fibers. 2019;7(4). https://doi.org/10.3390/fib7040033

5. Rajendra K, Babu M, Rao PG et al. Recent developments in the fabrication of metal matrix composites by stir casting route. A Review. Int J Chem Sci. 2016;14(4):2358-66. ISSN 0972-768X

6. Sankhla A, Patel KM. Metal matrix composites fabricated by stir casting process–a review. Adv Mater Process Technol. 2022;8(2):1270-91. https://doi.org/10.1080/2374068X.2020.1855404

7. Ibhadode AOA, Ebhojiaye RS. A new lightweight material for possible engine parts manufacture. Futur Intern Combust Engines. In: A New Lightweight Material for Possible Engine Parts Manufacture. 2018. https://doi.org/10.5772/intechopen.82268

8. Palanivendhan M, Nigam Y, Trivedi K. Experimental evaluation of aluminium alloy reinforced with silicon carbide. Int J Appl Eng Res. 2015;10(91):44-48.

9. Vijayakumar S, Soundarrajan M, Palani SP et al. Studies on mechanical properties of Al-SiC metal matrix composite. Int J Mater Sci Eng. 2016;2(6):1-5. https://doi.org/10.14445/23948884/IJMSE-V2I6P101

10. Sharma P, Kumar BA. Development of mechanical and metallurgical behavior of Al-Sic reinforced metal matrix composite. Inter J Adv Eng Res Applic. 2016;2(4). ISSN: 2454-2377.

11. Reddy AC, Zitoun E. Matrix Al-alloys for silicon carbide particle reinforced metal matrix composites. Ind J Sci Technol. 2010;3(12):1184-7. https://doi.org/10.17485/ijst/2010/v3i12/29857

12. Singh A, Chaurasia R, Kumar C. Review on aluminium silicon carbide metal matrix composite. Int J Eng Res Technol. 2019;8(12):611-3. https://doi.org/10.17577/IJERTV8IS120329

13. Sadeghi B, Cavaliere P, Shabani A. Design strategies for enhancing strength and toughness in high performance metal matrix composites: A review. Mater Today Commun. 2023;37:107535. https://doi.org/10.1016/j.mtcomm.2023.107535

14. Grilo J, Carneiro VH, Teixeira JC et al. Manufacturing methodology on casting-based aluminium matrix composites: systematic review. Metals. 2021;11(3):436. https://doi.org/10.3390/met11030436

15. Sharma J, Nayak C, Chauhan PS et al. Studies and scientific research analysis of aluminium (Al7075) metal matrix composite surface morphology. Mater Tod Proc. 2024;103:388-393. https://doi.org/10.1016/j.matpr.2023.09.032

16. Behera RK, Samal BP, Panigrahi SC et al. Microstructural and mechanical analysis of sintered powdered aluminium composites. Adv Mater Sci Eng. 2020;2:1-7. https://doi.org/10.1155/2020/1893475

17. Emamy M, Razaghian A, Lashgari HR et al. The effect of Al–5Ti–1B on the microstructure, hardness and tensile properties of Al2O3 and SiC-containing metal–matrix composites. Mater Sci Eng A. 2008;485(1-2):210-7. https://doi.org/10.1016/j.msea.2007.07.090

18. Reddy AC, Zitoun E. Matrix al-alloys for alumina particle reinforced metal matrix composites. Ind Found J. 2009;55(1):21-24.

19. Yigezu BS, Mahapatra MM, Jha PK. Influence of reinforcement type on microstructure, hardness and tensile properties of an aluminum alloy metal matrix composite. J Miner Mater Charact Eng. 2013;01(04):124-130. https://doi.org/10.4236/jmmce.2013.14022

20. Alaneme KK, Bodunrin AM. Corrosion Behavior of Alumina Reinforced Aluminium (6063) Metal Matrix Composites. J Miner Mater Charact Eng. 2011;10(12):1153-1165. https://doi.org/10.4236/jmmce.2011.1012088

21. Senthil S, Raguraman M, Manalan DT. Manufacturing processes and recent applications of aluminium metal matrix composite materials: A review. Mater Tod Proceed. 2021;45(4):5934-5938. https://doi.org/10.1016/j.matpr.2020.08.792

22. Zhang C, Yao D, Yin J et al. Microstructure and mechanical properties of aluminum matrix composites reinforced with pre-oxidized β-Si3N4 whiskers. Mater Sci Eng A. 2018;723:109-117. https://doi.org/10.1016/j.msea.2018.03.038

23. Akbar HI, Surojo E, Ariawan D. Investigation of industrial and agro wastes for aluminum matrix composite reinforcement. Proced Struct Integr. 2020;27:30-7. https://doi.org/10.1016/j.prostr.2020.07.005

24. Joseph OO, Sivaprasad S, Singh R. Effect of Nano2 in Corrosion Inhibition of Micro-Alloyed Steel in E20 and E40 Simulated Fuel Grade Ethanol Environment. Conference: Materials Science and Technology. USA. 2019. https://doi.org/10.7449/2019/MST_2019_730_736

25. Olaniran O, Uwaifo O, Bamidele E et al. An investigation of the mechanical properties of organic silica, bamboo leaf ash and rice husk reinforced aluminium hybrid composite. Mater Sci Eng Int J. 2019;3(4):129-34. https://doi.org/10.15406/mseij.2019.03.00103

26. Bodunrin MO, Oladijo OP, Daramola OO et al. Porosity Measurement and Wear Performance of Aluminium Hybrid Composites Reinforced with Silica Sand and Bamboo Leaf Ash. Ann Fac Eng Huned-Inter J Eng. 2016;14(1):231:238. ISSN: 1584-2665.

27. Kumar BP, Birru AK. Microstructure and mechanical properties of aluminium metal matrix composites with addition of bamboo leaf ash by stir casting method. Trans Nonf Met Soc China. 2017;27(12):2555-72. https://doi.org/10.1016/S1003-6326(17)60284-X

28. Alaneme K, Ademilua BO, Bodunrin MO. Mechanical properties and corrosion behaviour of aluminium hybrid composites reinforced with silicon carbide and bamboo leaf ash. Tribol Ind. 2013;35(1):25-35. Corpus ID: 136546311.

29. Subrahmanyam A, Narsaraju G, Rao BS. Effect of rice husk ash and fly ash reinforcements on microstructure and mechanical properties of aluminium alloy (AlSi10Mg) matrix composites. Int J Adv Sci Technol. 2015;76:1-8. https://doi.org/10.14257/ijast.2015.76.01

30. Saravanan SD, Kumar MS. Effect of mechanical properties on rice husk ash reinforced aluminum alloy (AlSi10Mg) matrix composites. Proced Eng. 2013;64:1505-13. https://doi.org/10.1016/j.proeng.2013.09.232

31. Joseph OO, Dirisu JO, Atiba J et al. Mechanical and corrosive properties of AA7075 aluminium reinforced with rice husk ash particulates. Mater Res Express. 2023;10(11):116520. https://doi.org/10.1088/2053-1591/ad0dd3

32. Edoziuno FO, Odoni BU, Alo FI et al. Dry sliding wear and surface morphological examination of an aluminium matrix composite reinforced with palm kernel shell. Acta Metall Slov. 2020;26(2):54-62. https://doi.org/10.36547/ams.26.2.537

33. Oyedeji EO, Dauda M, Yaro SA et al. The effect of palm kernel shell ash reinforcement on microstructure and mechanical properties of Al-Mg-Si metal-matrix composites. Proc Inst Mech Eng Part C J Mech Eng Sci. 2021;236(3):1666-73. https://doi.org/10.1177/09544062211014535

34. Oladele IO, Okoro AM. The effect of palm kernel shell ash on the mechanical properties of as-cast aluminium alloy matrix composites. Leonar J Sci. 2016;28:15-30. ISSN 1583-0233.

35. Edoziuno FO, Adediran AA, Odoni BU et al. Physico-chemical and morphological evaluation of palm kernel shell particulate reinforced aluminium matrix composites. Mater Today Proc. 2021;38:652-7. https://www.sciencedirect.com/science/article/pii/S2214785320324238

36. Ikele US, Alaneme KK, Oyetunji A. Mechanical behaviour of stir cast aluminum matrix composites reinforced with silicon carbide and palm kernel shell ash. Manuf Rev. 2022;9:12. https://doi.org/10.1051/mfreview/2022011

37. Fayomi OSI, Atayero AA, Mubiayi MP et al. Mechanical and opto-electrical response of embedded smart composite coating produced via electrodeposition technique for embedded system in defence application. J Allo Comp. 2019;773:305-13. https://doi.org/10.1016/j.jallcom.2018.09.191

38. Islam A, Dwivedi SP, Yadav R et al. Development of aluminium based composite by utilizing industrial waste and agro-waste material as reinforcement particles. J Inst Eng Ser D. 2021;102(13):317-30. https://doi.org/10.1007/s40033-021-00292-z

39. Ajibola WA, Fakeye AB. Production and Characterization of ZincAluminium, Silicon Carbide Reinforced with Palm Kernel Shell Ash. Int J Eng Trends Technol. 2016;41(6):318-25. https://doi.org/10.14445/22315381/IJETT-V41P259

40. Atiba JO, Fayomi OSI. Study of multifaceted eco-friendly nanoparticle zinc coating incorporation on mild steel. Resul Surf Interfa. 2024;17:100293. https://doi.org/10.1016/j.rsurfi.2024.100293

41. Derek AO, Fayomi OSI, Atiba JO. Microstructural Characterization, Mechanical Performance and Anti-Corrosive Response of Zinc Multifaceted Coating on Mild Steel. Key Eng Mater. 2024;981:3-14. https://doi.org/10.4028/p-S6S0Ms

42. Omoegun OG, Fayomi OSI, Atiba JO. Investigation of the corrosive behavior and adsorption parameters of copper in a cowbone ash inhibited alkaline environment. J Bio- Tribo-Corrosion. 2023;9(4):75. https://doi.org/10.1007/s40735-023-00794-1

43. Khodabakhshi F, Simchi A. The role of microstructural features on the electrical resistivity and mechanical properties of powder metallurgy Al-SiC-Al2O3 nanocomposites. Mater Des. 2017;130:26-36. https://doi.org/10.1016/j.matdes.2017.05.047

44. Cui X, Wu Y, Zhang G et al. Study on the improvement of electrical conductivity and mechanical properties of low alloying electrical aluminum alloys. Compos Part B Eng. 2017;110:381-7. https://doi.org/10.1016/j.compositesb.2016.11.04

45. Alaneme KK, Sanusi KO. Microstructural characteristics, mechanical and wear behaviour of rice husk ash–alumina–graphite hybrid reinforced aluminium based composites. Eng Sci Technol Int J. 2015;18(3):416-22. https://doi.org/10.1016/j.jestch.2015.02.003